

Polyhedral Maghemite Nanocrystals Prepared by a Flame Synthetic Method: Preparations, Characterizations, and Catalytic Properties

Nan Zhao,[†] Wei Ma,[‡] Zhimin Cui,[†] Weiguo Song,[†] Chuanlai Xu,^{†,*} and Mingyuan Gao^{†,*}

[†]Institute of Chemistry, CAS, Bei Yi Jie 2, Zhong Guan Cun, 100190 Beijing, China, and [‡]School of Food Science and Technology, State Key Laboratory of Food Science and Technology, Jiangnan University, Lihu Road 1800, 214122 Wuxi, China

As the special properties of inorganic nanocrystals are strongly associated with the particle size and shape, over the past decades, different synthetic methods have been developed for producing nanometer-sized objects with great efforts being paid to the exploration of potentials for controlling the size and especially the shape of the resultant nanomaterials. From the thermodynamic point of view, the shape of a nanocrystal is strongly determined by the difference of free energies of various facets. Therefore, to effectively control the free energy of different facets by additives, or to force the free energies of different facets to be far away from those established under ambient conditions, is a very effective measure for controlling the shape of nanomaterials. In fact, both of these two strategies have widely been used in preparing different types of faceted nanomaterials. For example, anisotropic growth of nanocrystals achieved by selectively coating certain facets with different types of ligands is mainly based on the first strategy, while to achieve effective shape control by extreme preparative conditions such as high temperature or pressure can be classified in the second strategy.

Polyhedral nanoparticles as a special type of faceted nanomaterials have been demonstrated to possess unique properties associated with the facets, edges, and even corners.^{1–4} In the past decades, many kinds of polyhedral nanoparticles have been investigated; the most successful examples are seen from metal colloidal particles.⁵ Although polyhedral metal oxide nanocrystals can also be prepared *via* solution-based synthesis by facet-selective

ABSTRACT Highly uniform polyhedral γ -Fe₂O₃ nanocrystals are prepared *via* a flame synthesis method by directly combusting the organic solution of iron-precursor. Systematic investigations reveal that the polyhedral γ -Fe₂O₃ nanocrystals are 26-facet particles enclosed by six {100}, eight {111}, and twelve {110} facets, and these 26-facet γ -Fe₂O₃ nanocrystals present excellent catalytic activities associated with their polyhedral structures.

KEYWORDS: flame synthesis · polyhedral maghemite nanocrystals · morphology · catalytic properties

modification of ligand,^{6–11} the products are often a mixture of several different types of polyhedrons with many of them enclosed by a limited number of facets. Therefore, the synthesis of polyhedral nanoparticles which possess shape-related properties remains challenging.

Very recently, we have developed a new synthetic method for preparing nanomaterials with unusual morphologies by directly combusting an organic solution of metal-organic compounds.¹² In general, this synthetic method is similar to liquid-feed flame spray synthesis, but no gas is introduced to aerosolize the organic solution of the precursors while they are combusting. Even though the production rate is sacrificed in comparison with the latter method, the uniformity of the products is won. For example, a new type of iron oxide/silica composite particles (γ -Fe₂O₃||SiO₂) with an uniform Janus structure was successfully obtained by directly combusting a methanol solution of ferric triacetylacetonate (Fe(acac)₃) and tetraethyl orthosilicate (TEOS).¹² These results encourage us to further explore the potential of this new synthetic method in achieving nanomaterials with unique structures because flame offers a high temperature environment which

*Address correspondence to gaomy@iccas.ac.cn, xcl@jiangnan.edu.cn.

Received for review April 9, 2009 and accepted May 25, 2009.

Published online June 3, 2009. 10.1021/nn900364g CCC: \$40.75

© 2009 American Chemical Society

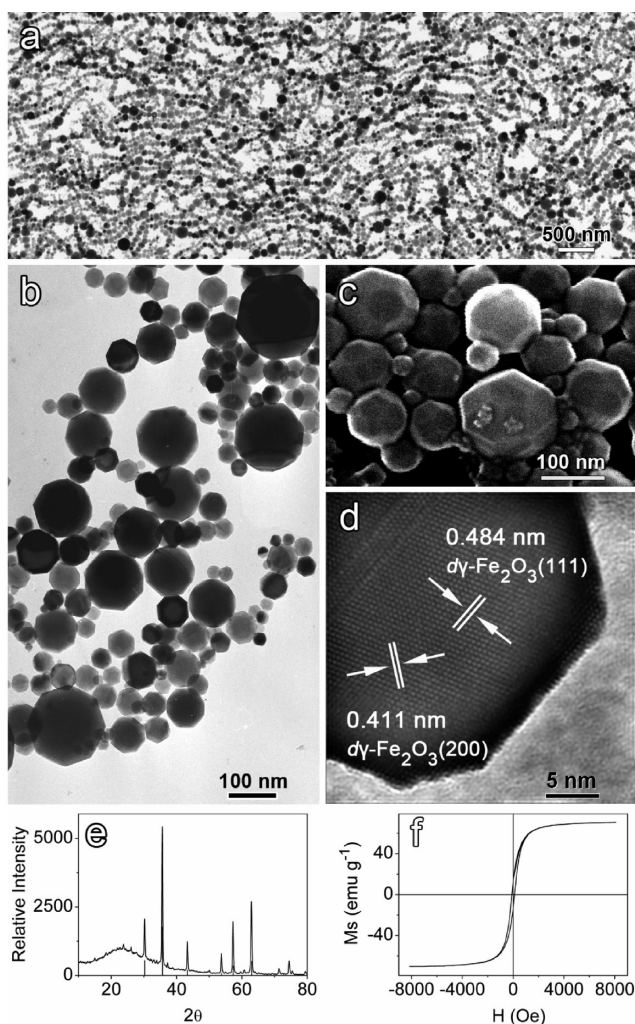


Figure 1. TEM images (a, b), SEM image (c) of the as-prepared nanoparticle sample, HRTEM image of a typical octagonal particle overlaid with identifications of crystal planes for $\gamma\text{-Fe}_2\text{O}_3$ (d), XRD patterns (e), and a room temperature hysteresis loop (f) of the as-prepared nanoparticle sample. The line patterns shown in panel e are the standard data for maghemite (JCPDS card 39-1346).

can never be achieved in solution-based synthesis.

Herein, we report a new type of polyhedral $\gamma\text{-Fe}_2\text{O}_3$ nanocrystals prepared by directly combusting a methanol solution of $\text{Fe}(\text{acac})_3$. Systematic experiments were performed to identify the morphology of the resultant polyhedral $\gamma\text{-Fe}_2\text{O}_3$ nanocrystals. Some preliminary experiments were carried out to further show the morphology-related special properties of the polyhedral $\gamma\text{-Fe}_2\text{O}_3$ nanocrystals.

RESULTS AND DISCUSSION

Preparation and Characterizations of the Polyhedral $\gamma\text{-Fe}_2\text{O}_3$ Nanocrystals. In general, the preparation of the $\gamma\text{-Fe}_2\text{O}_3$ nanoparticles was carried out according to the procedures reported before.¹² The main difference was that TEOS was not present in the system. In detail, the methanol solution of $\text{Fe}(\text{acac})_3$ (0.4 M) was prepared and used as precursor solution. During its combustion, a collecting procedure was started to harvest the nanoparticles formed in the flame.¹² Figure 1a shows a typi-

cal transmission electron microscopy (TEM) image of the nanocrystals collected from a flame envelope. The average particle size was determined to be 46 ± 25 nm. Interestingly, most of the nanoparticles present polygon shapes depicted by very clear outlines which can better be seen from an enlarged TEM image given in Figure 1b. In general, up to 95% of the polygons are of a highly symmetric octagon or hexagon shape. To further show the 3-dimensional structures of the polygons, scanning electron microscopy (SEM) investigations were performed. A typical SEM image given in Figure 1c shows that almost all particles are polyhedrons with a large number of facets. High-resolution transmission electron microscopy (HRTEM) and X-ray diffraction were adopted to further identify the crystalline structure of the polyhedrons shown in Figure 1c. The HRTEM image of a representative polyhedron overlaid with highlighted crystal shown in Figure 1d suggests that the polyhedrons are crystalline $\gamma\text{-Fe}_2\text{O}_3$ particles. The XRD patterns shown in Figure 1e reveal that all diffraction peaks match very well with those of bulk maghemite (JCPDS card 39-1346), which proves that the polyhedrons collected from the flame envelope are $\gamma\text{-Fe}_2\text{O}_3$ nanocrystals. Since the organic components of the precursor solution hardly survives in the flame envelope and since the temperature in the flame envelope is above 1000°C , the improved magnetic properties are expected from the resultant nanocrystals. The magnetic hysteresis curve presented in Figure 1f shows that the maghemite nanocrystals are ferromagnetic with a relatively small magnetic coercivity of 106 Oe. However, the room temperature saturation magnetization is around 71 emu g^{-1} , quite close to that of bulk maghemite,¹³ and much higher than those reported in literatures for nanometer-sized maghemite particles,^{14–16} which can partly be attributed to the high crystallinity degree achieved in the high temperature environment of the flame, besides the absence of organic coatings on the particle surface.

Identification of the Polyhedral Structure. It was also confirmed that the polyhedron structures were rather independent of the initial concentrations of $\text{Fe}(\text{acac})_3$, and lower $\text{Fe}(\text{acac})_3$ concentration was generally in favor of the formation of smaller maghemite nanocrystals. Although some flame-assisted syntheses of iron oxide nanoparticles have previously been reported,^{17–21} polygonal nanoparticles with a limited percentage was also observed and characterized by a platelet structure.^{20,21} As a matter of fact, maghemite nanocrystals with so many facets as shown in Figure 1c were not observed before. Therefore, it is necessary to clearly identify the polyhedral structure first. Representative polyhedrons are selected and shown in Figure 2. Close observation reveal that there only exist three sorts of facets on each single polyhedron, that is, octagon, hexagon, and tetragon. Their neighboring relationships are summarized as follows: one octagon neighbors four

hexagons and four tetragons, one hexagon contacts three octagons and three tetragons, and one tetragon borders two octagons and two hexagons. Therefore, two mathematics equations can be deduced by defining the number of octagons, hexagons, and tetragons on each particle as X , Y , Z , respectively. Since each hexagon provides three edges and each tetragon offers two edges to share with the neighboring octagons, the following eq 1 is established.

$$8X = 3Y + 2Z \quad (1)$$

Similarly, each octagon offers 4 edges and each tetragon provides 2 edges to share with the neighboring hexagons, then eq 2 is also true.

$$6Y = 4X + 2Z \quad (2)$$

Because each corner is formed by three different types of facets with respect to the current polyhedrons, the total number of corners and edges can be expressed by $(8X + 6Z + 4Z)/3$ and $(8X + 6Z + 4Z)/2$, respectively. According to the Euler's Formula for polyhedron (facets + corners = edges + 2), the following equation is established.

$$X + Y + Z + (8X + 6Z + 4Z)/3 = (8X + 6Y + 4Z)/2 + 2 \quad (3)$$

By solving eqs 1–3, the unique solution obtained is $X = 6$; $Y = 8$; $Z = 12$, which means one polyhedron contains six octagons, eight hexagons, and twelve tetragons. Therefore, the polyhedron prepared by the current synthetic route can be assigned to a great rhombicuboctahedron (26-facet polyhedron).

To further identify the facets, high magnification TEM images of three 26-facet polyhedrons with different orientations are carefully chosen to show in the lower panel of Figure 2. The corresponding selected-area electron diffraction (SAED) patterns of these polyhedrons are given in the middle column of the lower panel. As the polyhedrons have been demonstrated to be γ - Fe_2O_3 nanocrystals which possess a face-centered cubic (fcc) crystalline structure, according to the SAED results; the top facets on the 26-facet polyhedrons are consequently identified as $\{100\}$, $\{111\}$, and $\{110\}$ planes of γ - Fe_2O_3 , respectively. The clear outlines of the first and the third crystal shown in the lower panel allow a further measurement of the angles between identified facets. The three angles highlighted by black circles were determined to be 125° , 135° , and 145° , very well consistent with those for $\{100\} \wedge \{111\}$, $\{100\} \wedge \{110\}$, and $\{110\} \wedge \{111\}$ of fcc, which further confirms that the polyhedrons are of great rhombicuboctahedron.

Formation of 26-facet γ - Fe_2O_3 Nanocrystals in Fire. Although iron oxide polyhedral nanoparticles have been reported before, most of them are mainly formed by $\{100\}$ and $\{111\}$ facets except for some samples showing a limited number of $\{110\}$ facets.^{6–8} A polyhedral γ - Fe_2O_3 nanocrystal presenting as many as 12 $\{110\}$ facets has so far

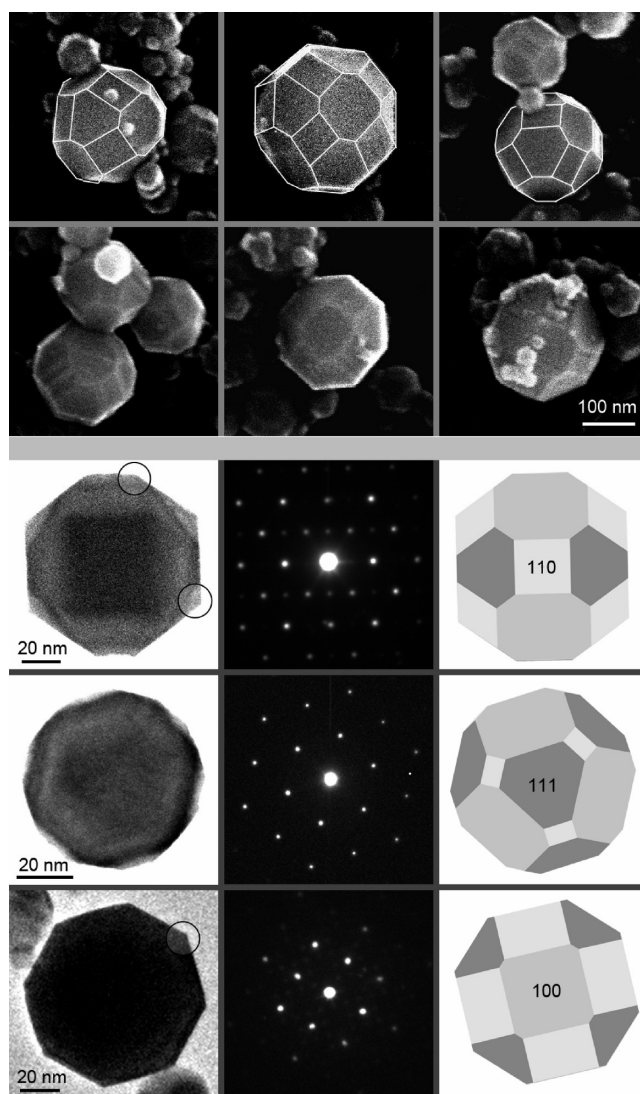


Figure 2. (Upper panel) SEM images of several typical polyhedral γ - Fe_2O_3 particles with highlighted edges; (lower panel) TEM images of three polyhedral γ - Fe_2O_3 particles with different orientations (left) together with their SAED patterns (middle) and the corresponding 2-dimensional models (right). The black circles in the lower panel highlights the angles formed by different facets, i.e., $\{100\} \wedge \{111\}$, $\{100\} \wedge \{110\}$, and $\{110\} \wedge \{111\}$.

not been reported yet. The facet analysis given in the first row of the lower panel of Figure 2 demonstrates that the $\{110\}$ facets present the largest distance to the crystal center in comparison with the $\{100\}$ and $\{111\}$ facets, which suggests that the $\{110\}$ facet possesses the highest surface energy according to a Wulff plot²² and explains the absence of $\{110\}$ facets in most γ - Fe_2O_3 nanocrystal samples. To monitor the formation of 26-facet γ - Fe_2O_3 nanocrystals in fire, three samples were collected using glass substrates covered by a thin layer of water from the flame cone, inner flame, and flame envelope, respectively. TEM and SAED results shown in Figure 3 revealed that in the flame cone small quasi-spherical particles with an average diameter of 20 nm were formed, while in the inner flame, these small particles greatly increased in size apart from the formation

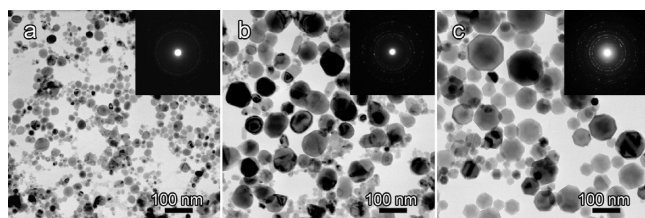


Figure 3. TEM images and SAED patterns of the samples collected from flame cone (a), inner flame (b), and flame envelope (c), respectively.

of crystalline phase, eventually they formed polyhedral nanocrystals in flame envelope with improved crystallinity degree as demonstrated by the SAED results. Since 26-facet γ - Fe_2O_3 nanocrystals are only found in the flame envelope where the temperature is above 1000 °C, it is reasonable to deduce that the ultrahigh reaction temperature may strongly influence the surface energy of {100}, {111}, and {110} facets by disturbing the relaxation of the atoms. Consequently, due to the fast quenching of the crystal growth by collecting the nanocrystals with flowing water, a large number of the unstable {110} facets with higher surface energy are preserved. This explanation can actually find support from a naturally occurring Martian meteorite in which 20-facet Fe_3O_4 crystals with 6 {110} facets were found.²³ Even though the appearance of different facets also strongly determined by the attachment of ligands in liquid phase synthesis, the influence of ligands on the eventual crystal shape is certainly not applicable for the current discussions.

Catalytic Properties of 26-Facet γ - Fe_2O_3 Nanocrystals. As the properties of a nanomaterial are strongly size- and shape-dependent,¹ it is interesting to further investigate the special properties of the current 26-facet γ - Fe_2O_3 nanocrystals. It was previously reported that γ - Fe_2O_3 nanoparticles can catalyze the oxidation of olefin to form aldehyde, a series of experiments were carried out to show the catalytic activities of the current polyhedral nanocrystals. A styrene-to-benzaldehyde conversion reaction was adopted as a model reaction.²⁴ Two commercial γ - Fe_2O_3 nanoparticle samples purchased from Beijing Fangshan Yihua Chemical factory (ref. No.: 0021215, sample 1) and Aldrich (No.: 544884-5G, sample 2) were used, respectively. As a matter of fact, the latter one (sample 2) was reported to have a very high selectivity in converting styrene to benzaldehyde, therefore the same recipe was also used as reported by Beller in their investigations, that is, 80 mg of γ - Fe_2O_3 (sample 1 or sample 2), 5.75 mL of styrene, 10 mL of H_2O_2 (30 wt %).²⁴ The reaction was performed at 75 °C. To more accurately compare the experimental results, the specific surface area of the 26-facet polyhedral nanocrystals (18.9 m^2/g), sample 1 (19.4 m^2/g), and sample 2 (43.1 m^2/g) was first determined by gas adsorption (BET) method. Then, two sets of experiments were carried out by calibrating the amount of the 26-facet γ - Fe_2O_3 nanocrystals according to the total sur-

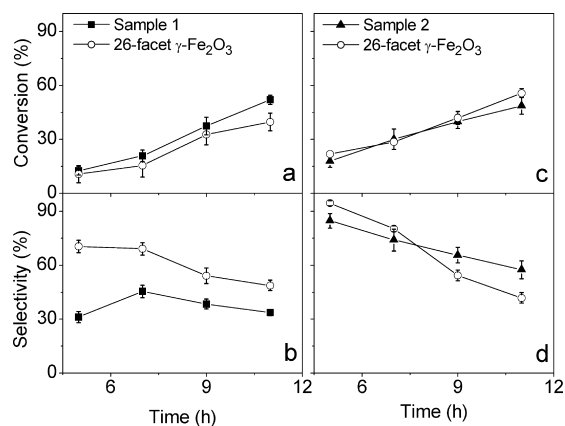


Figure 4. Selectivity and conversion of the styrene-to-benzaldehyde reaction as functions of reaction time. The results shown in frames a and b (the first set of experiments) were obtained by using 80 mg sample 1 and 78 mg 26-facet γ - Fe_2O_3 , respectively, while those shown in frames c and d (the second set of experiments) were obtained by using 80 mg sample 2 and 160 mg 26-facet γ - Fe_2O_3 , respectively. Note: In each set of experiments, the amount of 26-facet γ - Fe_2O_3 was normalized according to the total surface area of 80 mg commercial sample.

face areas of 80 mg samples 1 and 2, respectively. The detailed results of the first set of experiments shown in Figure 4a,b suggest that in comparison with sample 1 the 26-facet γ - Fe_2O_3 nanocrystals present much higher selectivities (1.5–2 times) in spite of slightly lower conversions in the inspected time window. In the second set of experiments, the 26-facet γ - Fe_2O_3 nanocrystals present rather comparable conversions within the first 10 h in comparison with sample 2, but higher selectivity (up to 95%) within the first 7 h of the reaction. The general decline of the selectivities for both 26-facet γ - Fe_2O_3 nanocrystals and sample 2 might be caused by selective adsorption of the products on the active facets. Owing to the difference in specific surface area between samples 1 and 2, the total surface area of the nanoparticle samples used in the second set of experiments was 2.2 times of those used in first set of experiments. Nevertheless, the results shown in Figure 4 panels d (second set of experiments) and b (first set of experiments) imply that sample 2 should also present higher selectivity than sample 1. Therefore, it is interesting to ask why 26-facet γ - Fe_2O_3 nanocrystals and sample 2 present enhanced catalytic selectivities.

In fact, the extraordinarily enhanced catalytic activities have been observed from faceted nanocrystals of noble metals,¹ and the appearances of high surface energy facets as well as more edges and corners were believed to be responsible. Therefore, the commercial γ - Fe_2O_3 nanocrystals, that is, samples 1 and 2, were studied by TEM. The results shown in Figure 5 reveal that sample 1 mainly consists of quasi-spherical particles forming irregularly shaped aggregates. In contrast, sample 2 presents morphologies rather similar to those of the 26-facet γ - Fe_2O_3 nanocrystals. There are nearly 65% particles being in hexagonal or octagonal

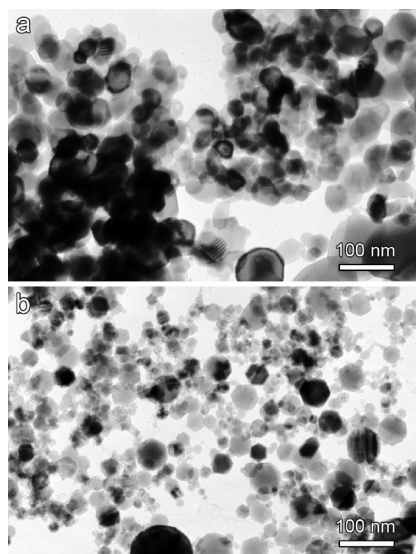


Figure 5. TEM images of the commercial $\gamma\text{-Fe}_2\text{O}_3$ nanoparticles: sample 1 (a) and sample 2 (b).

shapes. Moreover the size distribution of sample 2 is slightly larger due to the existence of very small spherical particles and some amorphous ones. Nevertheless, the similarity between the 26-facet $\gamma\text{-Fe}_2\text{O}_3$ nanocrystal sample and sample 2 and their enhanced selectivities suggest that the appearance of a huge number of facets, especially the $\{110\}$ facet should be responsible for the enhanced catalytic selectivity because the $\{110\}$ facet presents more Fe atoms than $\{100\}$ and $\{111\}$ in $\gamma\text{-Fe}_2\text{O}_3$.^{25,26} Because of the higher content of polyhedral particles in the current sample, under optimized conditions, the 26-facet $\gamma\text{-Fe}_2\text{O}_3$ nanocrystal sample presents a higher catalytic selectivity in comparison with sample 2, that is, 95% versus 85%. In addition, it is worth mentioning that because of the high saturation magnetization, the current 26-facet nanocrystal sample

presented very strong magnetic response. Ten seconds are enough to collect the nanocrystals by applying a 0.5 T magnet. Therefore, the 26-facet $\gamma\text{-Fe}_2\text{O}_3$ nanocrystals should have great potential for being used as a magnetically collectable catalyst. More systematic catalysis experiments are being performed to reveal the shape-related properties of the polyhedral $\gamma\text{-Fe}_2\text{O}_3$ nanocrystals.

CONCLUSIONS

The polyhedral $\gamma\text{-Fe}_2\text{O}_3$ nanocrystals with a uniform shape are prepared *via* the flame synthesis method by directly combusting the organic solution of iron-precursor. More detailed characterizations demonstrate that the polyhedral $\gamma\text{-Fe}_2\text{O}_3$ nanocrystals are of 26-facet particles enclosed by 6 $\{100\}$, 8 $\{111\}$, and 12 $\{110\}$ facets. Preliminary catalysis experiments reveal that the 26-facet $\gamma\text{-Fe}_2\text{O}_3$ nanocrystals present excellent catalytic activities with very high catalytic selectivities, which should be the direct result of the large number of different facets, especially the $\{110\}$ facets appearing on each nanocrystal. The current results as well as those reported in ref 12 also suggest that there are great varieties of nanomaterials existing in fire smokes, while the combustion of metal-containing flammable materials has strong reason to generate metal oxides nanomaterials. Therefore, it may be prudent to pay more attention to the investigation of the cytotoxicity of metal oxide nanomaterials as well as their interactions with air/blood barrier in human lung to gain new insight into the harmfulness of the fire smokes of nature disasters. Although the current investigations suggest that nanometer-sized particles are present in fire, they do hold great tendency to agglomerate forming larger aggregates of micrometers which are able to reach the deep territories of the lungs.

METHODS

Materials. $\text{Fe}(\text{acac})_3$ was purchased from F&F Chemical Co, Ltd. and used after a 2-fold recrystallization. Styrene, methanol, and H_2O_2 (30 wt %) were purchased from Beijing Fine Chemicals Co, Ltd. Styrene was used after reduced-pressure distillation.

Synthesis of Polyhedral $\gamma\text{-Fe}_2\text{O}_3$ Nanocrystals. $\text{Fe}(\text{acac})_3$ was selected as the precursor for maghemite, while methanol was used as both solvent and fuel. In a typical preparation, the concentration of $\text{Fe}(\text{acac})_3$ was 0.4 mol/L. After ignition of the precursor solution, nanoparticles were collected from the flame envelope by using a rotating glass tube covered by a thin layer of flowing water. More details can be found in one of our previous publications.

Styrene-to-Benzaldehyde Conversion Reaction. The styrene-to-benzaldehyde reaction was carried out as follows. Typically, 5.75 mL (50 mmol) of styrene, 10 mL of H_2O_2 (30 wt %), and 80 mg of commercial $\gamma\text{-Fe}_2\text{O}_3$ particles (0.5 mmol) were mixed under vigorous stirring and then allowed to react at 75 °C. Aliquots were extracted at 5, 7, 9, and 11 h. The conversion and selectivity were determined by analyzing volatile compounds in the reaction systems using gas chromatography equipped with a flame ionization detection facility. The specific surface area of the 26-facet polyhedral nanocrystals (18.9 m^2/g), sample 1 (19.4

m^2/g), and sample 2 (43.1 m^2/g) was determined by gas adsorption (BET) method. Taking the difference of the specific surface area of different $\gamma\text{-Fe}_2\text{O}_3$ samples into consideration, two different amounts of the 26-facet nanocrystals were used to enable comparable experimental results, that is, 78 mg for comparing with sample 1 and 160 mg for comparing with sample 2.

Characterizations. Low-resolution TEM images and selected area electron diffraction (SAED) patterns were recorded with a JEM-100CXII electron microscope operating at an accelerating voltage of 100 kV. High-resolution TEM (HRTEM) was accomplished using a FEI Tecnai20 at an accelerating voltage of 200 kV. Powder X-ray diffraction was measured with a Regaku D/Max-2500 diffractometer equipped with a $\text{Cu K}\alpha 1$ radiation ($\lambda = 1.54056 \text{ \AA}$). The hysteresis loops were recorded with the aid of vibrating sample magnetometer (VSM JDM-13, China). The specific surface area was measured by ST-2000 BET surface area analyzer. Agilent 6890 gas chromatography equipped with a 50-m capillary column and a FI (flame ionization) detector, and the published response factors were adopted for the catalysis experiments.

Acknowledgment. The current investigations were partly supported by NSFC projects (20673128, 20640430564, 20871060,

20835006) and a MPH project (2008ZX10001-014). The authors thank Dr. Min Gao for his kind help with HRTEM measurements.

REFERENCES AND NOTES

- Tian, N.; Zhou, Z. Y.; Sun, S. G.; Ding, Y.; Wang, Z. L. Synthesis of Tetrahedral Platinum Nanocrystals with High-Index Facets and High Electro-Oxidation Activity. *Science* **2007**, *316*, 732–735.
- Zhang, J. G.; Gao, Y.; Alvarez-Puebla, R. A.; Buriak, J. M.; Fenniri, H. Synthesis and SERS Properties of Nanocrystalline Gold Octahedra Generated from Thermal Decomposition of HAuCl₄ in Block Copolymers. *Adv. Mater.* **2006**, *18*, 3233–3237.
- Zheng, Y. H.; Cheng, Y.; Wang, Y. S.; Bao, F.; Zhou, L. H.; Wei, X. F.; Zhang, Y. Y.; Zheng, Q. Quasicyclic Alpha-Fe₂O₃ Nanoparticles with Excellent Catalytic Performance. *J. Phys. Chem. B* **2006**, *110*, 3093–3097.
- Kim, F.; Connor, S.; Song, H.; Kuykendall, T.; Yang, P. D. Platonic Gold Nanocrystals. *Angew. Chem., Int. Ed.* **2004**, *43*, 3673–3677.
- Tao, A. R.; Habas, S.; Yang, P. D. Shape Control of Colloidal Metal Nanocrystals. *Small* **2008**, *4*, 310–325.
- Cheon, J. W.; Kang, N. J.; Lee, S. M.; Lee, J. H.; Yoon, J. H.; Oh, S. J. Shape Evolution of Single-Crystalline Iron Oxide Nanocrystals. *J. Am. Chem. Soc.* **2004**, *126*, 1950–1951.
- Ahnyaz, A.; Skamoto, Y.; Bergstrom, L. Magnetic Field-Induced Assembly of Oriented Superlattices from Maghemite Nanocubes. *Proc. Natl. Acad. Sci. U.S.A.* **2007**, *104*, 17570–17574.
- Sun, S.; Zeng, H.; Robinson, D. B.; Raoux, S.; Rice, P. M.; Wang, S. X.; Li, G. Monodisperse MFe₂O₄ (M = Fe, Co, Mn) Nanoparticles. *J. Am. Chem. Soc.* **2004**, *126*, 273–279.
- Sun, Y. G.; Xia, Y. N. Shape-Controlled Synthesis of Gold and Silver Nanoparticles. *Science* **2002**, *298*, 2176–2179.
- Zhang, J.; Ohara, S.; Umetsu, M.; Naka, T.; Hatakeyama, Y.; Adschiri, T. Colloidal Ceria Nanocrystals: A Tailor-Made Crystal Morphology in Supercritical Water. *Adv. Mater.* **2007**, *19*, 203–206.
- Zheng, R.; Gu, H.; Xu, B.; Fung, K. K.; Zhang, X.; Ringer, S. P. Self-Assembly and Self-Oriented Truncated Octahedral Magnetite Nanocrystals. *Adv. Mater.* **2006**, *18*, 2418–2421.
- Zhao, N.; Gao, M. Y. Magnetic Janus Particles Prepared by a Flame Synthetic Approach: Synthesis, Characterizations, and Properties. *Adv. Mater.* **2009**, *21*, 184–187.
- Liu, Z. L.; Wang, H. B.; Lu, Q. H.; Du, G. H.; Peng, L.; Du, Y. Q.; Zhang, S. M.; Yao, K. L. Synthesis and Characterization of Ultrafine Well-Dispersed Magnetic Nanoparticles. *J. Magn. Mater.* **2004**, *283*, 258–262.
- Kang, Y. S.; Risbud, S.; Rabolt, J. F.; Stroeve, P. Synthesis and Characterization of Nanometer-Size Fe₃O₄ and Gamma-Fe₂O₃ Particles. *Chem. Mater.* **1996**, *8*, 2209–2211.
- Woo, K.; Hong, J.; Choi, S.; Lee, H. W.; Ahn, J. P.; Kim, C. S.; Lee, S. W. Easy Synthesis and Magnetic Properties of Iron Oxide Nanoparticles. *Chem. Mater.* **2004**, *16*, 2814–2818.
- Roca, A. G.; Marco, J. F.; Morales, M. D.; Serna, C. J. Effect of Nature and Particle Size on Properties of Uniform Magnetite and Maghemite Nanoparticles. *J. Phys. Chem. C* **2007**, *111*, 18577–18584.
- Zachariah, M. R.; Aquino, M. I.; Shull, R. D.; Steel, E. B. Formation of Superparamagnetic Nanocomposites from Vapor Phase Condensation in a Flame. *Nanostruct. Mater.* **1995**, *5*, 383–392.
- Janzen, C.; Roth, P. Formation and Characteristics of Fe₂O₃ Nano-Particles in Doped Low Pressure H₂/O₂/Ar Flames. *Combust. Flame* **2001**, *125*, 1150–1161.
- Grimm, S.; Schultz, M.; Barth, S.; Muller, R. Flame Pyrolysis—A Preparation Route for Ultrafine Pure γ -Fe₂O₃ Powders and the Control of Their Particle Size and Properties. *J. Mater. Sci.* **1997**, *32*, 1083–1092.
- Li, D.; Teoh, W. Y.; Selomulya, C.; Woodward, R. C.; Amal, R.; Rosche, B. Flame-Sprayed Superparamagnetic Bare and Silica-Coated Maghemite Nanoparticles: Synthesis, Characterization, and Protein Adsorption-Desorption. *Chem. Mater.* **2006**, *18*, 6403–6413.
- Li, D.; Teoh, W. Y.; Selomulya, C.; Woodward, R. C.; Munroe, P.; Amal, R. Insight into Microstructural and Magnetic Properties of Flame-Made γ -Fe₂O₃ Nanoparticles. *J. Mater. Chem.* **2007**, *17*, 4876–4884.
- Metois, J. J.; Muller, P. Absolute Surface Energy Determination. *Surf. Sci.* **2004**, *548*, 13–21.
- Golden, D. C.; Ming, D. W.; Morris, R. V.; Brearley, A.; Lauer, H. V.; Treiman, A. H.; Zolensky, M. E.; Schwandt, C. S.; Lofgren, G. E.; McKay, G. A. Evidence for Exclusively Inorganic Formation of Magnetite in Martian Meteorite ALH84001. *Am. Mineral.* **2004**, *89*, 681–695.
- Shi, F.; Tse, M. K.; Pohl, M.; Bruchner, A.; Zhang, S.; Beller, M. Tuning Catalytic Activity between Homogeneous and Heterogeneous Catalysis: Improved Activity and Selectivity of Free Nano-Fe₂O₃ in Selective Oxidations. *Angew. Chem., Int. Ed.* **2007**, *46*, 8866–8868.
- Baetzold, R. C.; Yang, H. Computational Study on Surface Structure and Crystal Morphology of Gamma-Fe₂O₃: Toward Deterministic Synthesis of Nanocrystals. *J. Phys. Chem. B* **2003**, *107*, 14357–14364.
- Costas, M.; Chen, K.; Que, Jr. L. Biomimetic Nonheme Iron Catalysts for Alkane Hydroxylation. *Coord. Chem. Rev.* **2000**, *200–202*, 517–544.